Mutations in *TFAP2B* and previously unimplicated genes of the BMP, Wnt, and Hedgehog pathways in syndromic craniosynostosis

Andrew T. Timberlake[a,b,c,d], Sheng Chih Jin[a,d], Carol Nelson-Williams[a,d], Robin Wu[c], Charuta G. Furey[a], Barira Islam[e,f], Shozeb Haider[e], Erin Loring[a], Amy Galm[g], Yale Center for Genome Analysis[1], Derek M. Steinbacher[c], Dawid Larysz[h], David A. Staffenberg[b], Roberto L. Flores[b], Eduardo D. Rodriguez[b], Titus J. Boggon[i], John A. Persing[c], and Richard P. Lifton[a,d,2]

[a]Department of Genetics, Yale University School of Medicine, New Haven, CT 06510; [b]Hansjörg Wyss Department of Plastic Surgery, New York University Langone Medical Center, New York, NY 10016; [c]Section of Plastic and Reconstructive Surgery, Yale University School of Medicine, New Haven, CT 06510; [d]Laboratory of Human Genetics and Genomics, The Rockefeller University, New York, NY 10065; [e]School of Pharmacy, University College London, London WC1N 1AX, United Kingdom; [f]Centre for Biomarker Research, School of Applied Sciences, University of Huddersfield, Queensgate, Huddersfield HD1 3DH, United Kingdom; [g]Craniosynostosis and Positional Plagiocephaly Support, New York, NY 10010; [h]Department of Radiotherapy, The Maria Skłodowska Curie Memorial Cancer Centre and Institute of Oncology, 44-101 Gliwice, Poland; and [i]Department of Pharmacology, Yale University, New Haven, CT 06510

Contributed by Richard P. Lifton, June 11, 2019 (sent for review February 4, 2019; reviewed by Sekar Kathiresan and Yuji Mishina)

Craniosynostosis (CS) is a frequent congenital anomaly featuring the premature fusion of 1 or more sutures of the cranial vault. Syndromic cases, featuring additional congenital anomalies, make up 15% of CS. While many genes underlying syndromic CS have been identified, the cause of many syndromic cases remains unknown. We performed exome sequencing of 12 syndromic CS cases and their parents, in whom previous genetic evaluations were unrevealing. Damaging de novo or transmitted loss of function (LOF) mutations were found in 8 genes that are highly intolerant to LOF mutation ($P = 4.0 \times 10^{-8}$); additionally, a rare damaging mutation in *SOX11*, which has a lower level of intolerance, was identified. Four probands had rare damaging mutations (2 de novo) in *TFAP2B*, a transcription factor that orchestrates neural crest cell migration and differentiation; this mutation burden is highly significant ($P = 8.2 \times 10^{-12}$). Three probands had rare damaging mutations in *GLI2*, *SOX11*, or *GPC4*, which function in the Hedgehog, BMP, and Wnt signaling pathways; other genes in these pathways have previously been implicated in syndromic CS. Similarly, damaging de novo mutations were identified in genes encoding the chromatin modifier *KAT6A*, and *CTNNA1*, encoding catenin α-1. These findings establish *TFAP2B* as a CS gene, have implications for assessing risk to subsequent children in these families, and provide evidence implicating other genes in syndromic CS. This high yield indicates the value of performing exome sequencing of syndromic CS patients when sequencing of known disease loci is unrevealing.

craniosynostosis | de novo mutation | craniofacial syndromes | pleiotropy | TFAP2B

Craniosynostosis (CS) is one of the most frequent birth defects, occurring once in every 2,000 live births. Affected subjects typically require surgery early in life to allow normal growth of the developing brain, which doubles in volume in the first year. Syndromic CS cases, featuring additional extracranial anomalies, make up ∼15% of cases. Rare Mendelian mutations in more than 40 genes have been found to underlie syndromic CS. These genes are highly clustered in several developmental signaling cascades, including the BMP, Wnt, Ras/ERK, ephrin, hedgehog, STAT, and retinoic acid pathways (1–3). Collectively, the pleiotropic effects of syndromic mutations affect virtually all organ systems, with the limbs and cardiovascular system most commonly involved (1). Clinical manifestations are highly variable among affected individuals even in syndromes caused by recurrent mutations (e.g., Apert, Muenke, Pfeiffer syndromes), demonstrating the variable expressivity of these mutations (1). The diagnostic utility of screening for mutations or copy number variants at known disease loci is quite high in syndromic CS, with recent studies establishing a molecular diagnosis in >70% of cases studied (4). Nonetheless, testing frequently remains unrevealing, despite often striking clinical presentations. Given the high prevalence of rare mutations with large effect in these syndromic cases, we posited that mutation-negative syndromic probands would be an excellent source for identification of genes causing premature closure of cranial sutures. We anticipated that disease-related mutations in outbred families would likely be recognized as de novo or rare transmitted damaging mutations in genes intolerant to loss of function (LOF) mutation (high probability of LOF intolerance [pLI]) and in pathways previously implicated in CS (see above) or other congenital malformations (e.g., chromatin modification) (3, 5–7).

Significance

Craniosynostosis (CS) is a frequent congenital malformation featuring premature fusion of cranial sutures; 15% of these children have syndromic disease, often due to rare mutations with large effect. While many genes causing Mendelian forms of syndromic CS have been identified, clinical sequencing often fails to identify a likely causative mutation. We performed whole-exome sequencing of 12 case-parent trios with previously negative genetic evaluations. The results identified likely pathogenic mutations in *TFAP2B*, *KAT6A*, *GLI2*, *SOX11*, *CTNNA1*, and *GPC4* in these families, adding several loci to those known to cause syndromic CS. The findings have implications for determining risk of disease in subsequent offspring and demonstrate that unexplained syndromic CS cases are a particularly rich vein for discovery of CS loci.

Author contributions: A.T.T. and R.P.L. conceived, designed, and directed study; A.T.T., E.L., and A.G. recruited and enrolled patients; A.T.T. collected genetic specimens; A.T.T., S.C.J., C.N.-W., R.W., C.G.F., and R.P.L. performed genetic analyses; B.I. and S.H. generated structural models of mutant alleles; Yale Center for Genome Analysis directed exome sequence production; D.M.S., D.L., D.A.S., R.L.F., E.D.R., and J.A.P. contributed clinical evaluations; T.J.B. generated structural models of wild-type and mutant alleles; and A.T.T. and R.P.L. wrote the paper.

Reviewers: S.K., Massachusetts General Hospital; and Y.M., University of Michigan.

The authors declare no conflict of interest.

Data deposition: Exome sequence data for case-parent trios have been deposited in the NCBI database of Genotypes and Phenotypes (dbGaP) (accession no. phs000744).

[1]A complete list of the Yale Center for Genome Analysis can be found in *SI Appendix*.

[2]To whom correspondence may be addressed. Email: rickl@mail.rockefeller.edu.

This article contains supporting information online at www.pnas.org/lookup/suppl/doi:10.1073/pnas.1902041116/-/DCSupplemental.

Published online July 10, 2019.

Results

Damaging De Novo Mutations in Syndromic CS. We ascertained 12 probands with syndromic CS, all of whom had undergone reconstructive surgery for CS, who had negative genetic studies in clinical laboratories. Prior evaluations included sequencing of prevalent syndromic loci in all probands (*SI Appendix*, Table S1) and assessment of copy number variants identified via array comparative genomic hybridization in 9 probands. We also searched for rare damaging mutations in *SMAD6* implicated in nonsyndromic CS (2) but found none in these kindreds. Clinical features of these probands are described in *SI Appendix*, Table S2. Exome sequencing was performed as previously described (3), with 98.6% of all RefSeq coding bases and splice junctions having 8 or more independent reads and median coverage of 42. We identified de novo likely LOF and damaging missense mutations (per metaanalytic support vector machine [MetaSVM]) as well as rare (minor allele frequency [MAF] $< 2 \times 10^{-5}$) transmitted damaging heterozygous or hemizygous mutations. We also identified recessive damaging genotypes with each contributing allele having an allele frequency $<10^{-3}$. Mutations contributing to statistically significant results were confirmed by Sanger sequencing of PCR products containing the variant site amplified from genomic DNA; these variants are described in Dataset S1.

Analysis of the distribution of de novo mutations showed that there were 6 damaging de novo mutations among the 3,320 genes that are highly intolerant to LOF mutations (pLI $\geq$ 0.9) (8), significantly more than expected by chance (6.12-fold enrichment, 1-tailed Poisson $P = 5.4 \times 10^{-4}$) (Table 1).

***TFAP2B* Mutations in Syndromic CS.** We found 2 damaging de novo mutations in *TFAP2B*: a canonical splice donor site mutation in the third intron (IVS3 + 2T > A) and a missense mutation p.K276R. Both mutations were absent in Exome Aggregation Consortium (ExAC) (9). The probability of observing 2 damaging de novo mutations in *TFAP2B* in a cohort of this size was 7.7×10^{-8} (Poisson test), well surpassing the threshold for genome-wide significance (2.6×10^{-6}). We also found 2 rare transmitted LOF mutations in *TFAP2B*: a p.R382X premature termination mutation and a p.M1I start loss mutation (Table 2). These mutations are absent in >100,000 alleles in ExAC (9). The probability of observing 2 damaging de novo (1 of these being LOF) and 2 transmitted LOFs in this small cohort by chance was highly unlikely ($P = 8.2 \times 10^{-12}$ by Poisson distribution and binomial test, combined using Fisher's method) (*Methods*).

Table 1. Enrichment of damaging de novo mutations in syndromic CS cases but not controls

	Observed		Expected			
Mutation class	*N*	Rate	*N*	Rate	Enrichment	*P* value
Cases = 12, offspring studied = 13						
All genes						
Total	14	1.08	14.83	1.14	0.94	0.62
Syn	2	0.15	4.12	0.32	0.48	0.92
T-Mis	4	0.31	7.42	0.57	0.54	0.94
D-Mis	4	0.31	1.71	0.13	2.34	0.09
LOF	3	0.23	1.28	0.10	2.35	0.14
In-frame indels	1	0.08	0.30	0.02	3.36	0.26
Damaging	8	0.62	3.29	0.25	2.43	0.02
LOF-intolerant genes (pLI greater than or equal to 0.9)						
Total	6	0.46	3.99	0.31	1.50	0.21
Syn	0	0.00	1.08	0.08	0.00	1.00
T-Mis	0	0.00	1.92	0.15	0.00	1.00
D-Mis	2	0.15	0.53	0.04	3.76	0.10
LOF	3	0.23	0.36	0.03	8.25	6.1×10^{-3}
In-frame indels	1	0.08	0.09	0.01	11.73	0.08
Damaging	6	0.46	0.98	0.08	6.12	5.4×10^{-4}
Controls = 1,789						
All genes						
Total	514	0.29	537.85	0.30	0.96	0.85
Syn	127	0.07	145.35	0.08	0.87	0.94
T-Mis	275	0.15	258.58	0.14	1.06	0.16
D-Mis	64	0.04	72.62	0.04	0.88	0.86
LOF	38	0.02	49.66	0.03	0.77	0.96
In-frame indels	10	0.01	11.64	0.01	0.86	0.73
Damaging	112	0.06	133.92	0.07	0.84	0.98
LOF-intolerant genes (pLI greater than or equal to 0.9)						
Total	514	0.29	537.85	0.30	0.96	0.85
Syn	127	0.07	145.35	0.08	0.87	0.94
T-Mis	275	0.15	258.58	0.14	1.06	0.16
D-Mis	64	0.04	72.62	0.04	0.88	0.86
LOF	38	0.02	49.66	0.03	0.77	0.96
In-frame indels	10	0.01	11.64	0.01	0.86	0.73
Damaging	112	0.06	133.92	0.07	0.84	0.98

LOF denotes premature termination, frameshift, or splice site mutation. Damaging includes LOF, D-Mis, and in-frame indels. *P* values represent the upper tail of the Poisson probability density function. Because the mutation in *GPC4* was de novo in the proband's mother, a total of 13 offspring were considered in the de novo mutation analysis for cases. D-Mis, damaging missense called by MetaSVM; *N*, number of de novo mutations; rate, number of de novo mutations per subject; Syn, synonymous; T-mis, tolerated missense called by MetaSVM.

Table 2. Likely pathogenic variants in probands with syndromic CS

Kindred identification	Type of CS	Gene	Impact	Inheritance	ExAC frequency	pLI
SAG249	Sagittal	*TFAP2B*	M1I (start loss)	Inherited (unaffected parent)	0	0.99
MET268	Metopic	*TFAP2B*	K276R	De novo	0	0.99
MET271	Metopic	*TFAP2B*	IVS3+2 T > A	De novo	0	0.99
MET117	Metopic	*TFAP2B*	R382X	Inherited (affected parent)	0	0.99
SAG250	Sagittal and etopic	*KAT6A*	E1221X	De novo	0	1
LAM108	Lambdoid	*SOX11*	R64H	De novo	0	0.34
PSAG38	Sagittal	*GLI2*	A551T	De novo	0	1
MET188	Metopic	*GPC4*	V152fs	De novo in mother	0	0.95
SAG359	Sagittal	*CTNNA1*	V374_375insSWKMK	De novo	0	0.97

TFAP2B is highly intolerant to LOF mutations, with none identified among >100,000 alleles in ExAC (9) (pLI = 0.99), making this result all of the more striking (3 LOFs in 12 probands vs. 0 in 60,706 ExAC controls, $P = 6.79 \times 10^{-12}$).

TFAP2B is a transcription factor involved in neural crest cell differentiation. Aberrant developmental signaling in cranial neural crest cells has been demonstrated to cause CS in several mouse models (10–12). Three probands had metopic synostosis (fusion of the frontal bones of the skull) with severe trigonocephaly (triangular skull); 2 of these had clinodactyly, and 1 had brachydactyly (congenital malformations of the fingers) (Fig. 1). The other subject who had a transmitted LOF mutation in *TFAP2B* had sagittal synostosis (fusion of the parietal bones) with severe scaphocephaly (long, narrow skull) and brachydactyly. A variety of other congenital abnormalities was seen (*SI Appendix*, Table S2). In 1 of these families (SAG249), the mutation-transmitting parent showed no signs of CS; however, in the second family (MET117), clinical examination of the transmitting father as well as analysis of his childhood photographs suggested uncorrected metopic synostosis.

Interestingly, heterozygous damaging mutations in *TFAP2B* have previously been implicated in Char syndrome, a syndromic form of patent ductus arteriosus often presenting with characteristic facies and limb anomalies (13). Notably, several patients with Char syndrome had abnormal head shapes and ridging over the cranial sutures, suggesting the possibility of CS (14), although this was not confirmed. In our patients with *TFAP2B* mutation, aside from clear demonstration of CS, several recurrent phenotypes not previously reported in Char syndrome were observed, including recurrent pulmonary and otolaryngeal infections (n = 2), hypovitaminosis D (n = 2), and severe growth and developmental delays (n = 2); additional traits observed in single probands not previously described were severe allergic rhinitis and asthma (n = 1), recurrent transaminitis, agenesis of the corpus callosum, seizures, and sensory processing disorder (*SI Appendix*, Table S2). Of the 3 probands in whom an echocardiogram was obtained, only 1 proband, who was asymptomatic, had a patent ductus arteriosus (PDA), which was monitored and resolved spontaneously by the age of 7. The phenotypes in these patients with *TFAP2B* mutations thus expand the range of phenotypes resulting from haploinsufficiency, highlighting the pleiotropy and variable expressivity resulting from these mutations.

We searched for rare (ExAC frequency < 2×10^{-5}) and damaging (LOF or MetaSVM-D missense) variants in *TFAP2B* in 485 previously sequenced probands with nonsyndromic sagittal or metopic CS (2, 3). This identified a single *TFAP2B* damaging missense mutation (p.Q8E, which has MAF = 0 in ExAC) transmitted from an unaffected parent. This proband had no extracranial anomalies, and the significance of this damaging missense variant in a nonsyndromic proband is uncertain. LOF and damaging missense mutations in *TFAP2B* thus seem to be highly enriched in syndromic CS probands in comparison with nonsyndromic probands.

De Novo Damaging Mutations Enriched in Known Disease Genes and High pLI Genes. Among the 8 remaining probands, we found de novo LOF or likely damaging mutations in 5 kindreds. Four of these mutations were in known Mendelian genes listed in Online Mendelian Inheritance in Man (OMIM; https://www.omim.org/) (Poisson $P = 7.8 \times 10^{-4}$; 9.98-fold enrichment) (*SI Appendix*, Table S3). Four of these genes had pLI > 0.90, which was not expected by chance (Poisson $P = 5.2 \times 10^{-3}$; 5.89-fold enrichment), while 1 had pLI = 0.34. Only 1 of these genes had any prior association with CS. Importantly, however, 3 of these genes lie in pathways frequently mutated in other syndromic forms of CS (BMP, Wnt, Ras/ERK, ephrin, hedgehog, STAT, and retinoic acid pathways as noted previously [1–3]). *GLI2*, *SOX11*, and *GPC4* lie in the hedgehog, BMP, and Wnt signaling pathways, respectively. Among these 8 kindreds, the probability of finding 3 damaging de novo mutations among the 963 genes of the BMP, Wnt, Ras/ERK, ephrin, hedgehog, STAT, and retinoic acid pathways (per gene ontology) by chance is 3.3×10^{-4} (enrichment 23-fold) (3). This result provides strong support for these mutations contributing to the pathogenesis of CS in these kindreds.

One proband had a de novo LOF mutation in *KAT6A*. The proband was born with combined sagittal and metopic synostosis

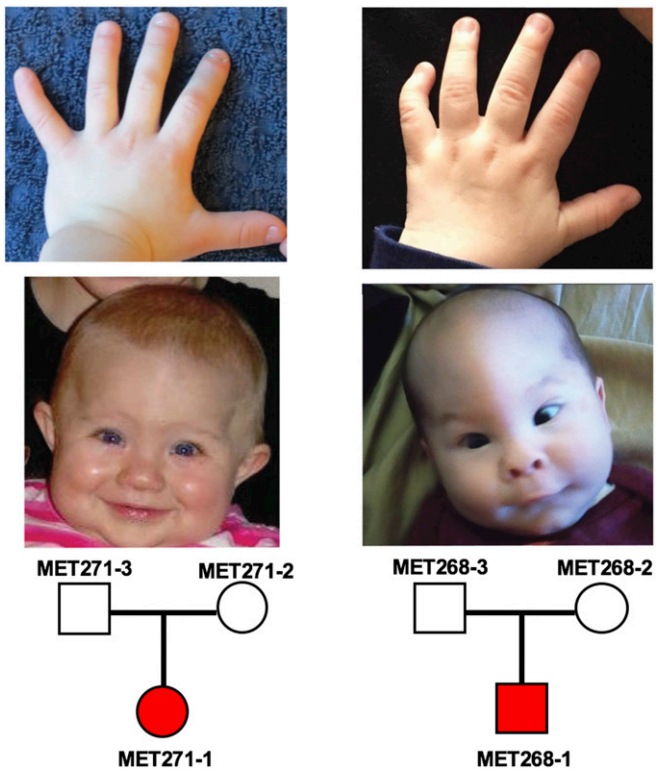

Fig. 1. Probands with de novo damaging mutations in *TFAP2B*. Hands and faces of the 2 probands as well as pedigrees from each kindred are demonstrated in each column. Patients were diagnosed with severe trigonocephaly in early infancy, with neonatal diagnoses of brachydactyly (MET271) or clinodactyly (MET268).

and had the de novo mutation p.E1221X. KAT6A encodes a histone acetyltransferase implicated in H3K9 and H3K18 acetylation and has a pLI of 1.0. De novo LOF mutations in this gene were previously reported in probands with complex syndromic intellectual disability and developmental delay (15, 16); 3 subjects from 1 study were reported to have midline CS (16). Many additional syndromic findings in our proband overlapped with findings in other reported KAT6A-mutant patients, including a patent ductus arteriosus, an atrial septal defect and patent foramen ovale, dysplastic mitral valve with mitral and tricuspid valve regurgitation, hypotonia, down-turned corners of the mouth, microgenia, an inverted nipple, bilateral clinodactyly of both fifth toes and mild 2- to 3-toe syndactyly, hemangiomas ($n = 10$) widely distributed across the body surface, oral feeding difficulties with nasogastric tube dependency, laryngomalacia, seizures, hypoplastic corpus callosum with white matter atrophy, bilateral cryptorchidism, and an underdeveloped scrotum (*SI Appendix*, Table S2). In addition, this child had several features not previously described, including bronchial atrophy involving the right mainstem and upper lobe bronchus, cupped and posteriorly rotated ears bilaterally, and the absence of tooth eruption at age 2. The extensive overlap of findings with other previously described cases leaves little doubt that the identified mutation is causally related to the phenotypes in this patient and provides evidence of additional expansion of the phenotypes resulting from haploinsufficiency for *KAT6A*. Consistent with this notion, no other de novo damaging mutations or LOF mutations in OMIM or high pLI genes were found in this proband.

A de novo mutation at a highly conserved residue in a highly conserved segment of *GLI2* (p.A551T) was identified in a child born with sagittal CS, neurogenic bladder, cerebral palsy, atrophy of the right optic nerve, hydrocephalus, absence of the right thumb, severe kyphosis, and scoliosis (Fig. 2 and *SI Appendix*, Table S2). No other likely de novo mutations were identified in this proband, and there were no transmitted damaging genotypes in high pLI genes or known OMIM genes identified in this proband. *GLI2* encodes a zinc finger transcription factor in the hedgehog signaling pathway and is highly intolerant to LOF mutation (pLI = 1.0). The identified variant lies within the fourth C2H2 zinc finger domain; the fourth and fifth zinc fingers mediate the binding of GLI2 to its cognate DNA sequence (17). The crystal structure of the close paralog encoded by GLI1, bound to its cognate DNA sequence, has been determined (Protein Data Bank [PDB] ID code 2GLI) (18). These proteins are highly homologous, including 92% sequence identity across the fourth zinc finger, with 100% identity across the 21-amino acid segment that contains the sequences that directly interact with DNA bases (amino acids 547 to 552) (*SI Appendix*, Fig. S1). Residue A551 is expected to lie in the center of the "Finger 4" motif, which recognizes the major groove; this alanine is predicted to abut the adjacent nucleotide (Fig. 2*G*). Substitution of the larger and hydrophilic threonine mutation is highly likely to deleteriously impact, or alter, the binding of GLI2 to DNA.

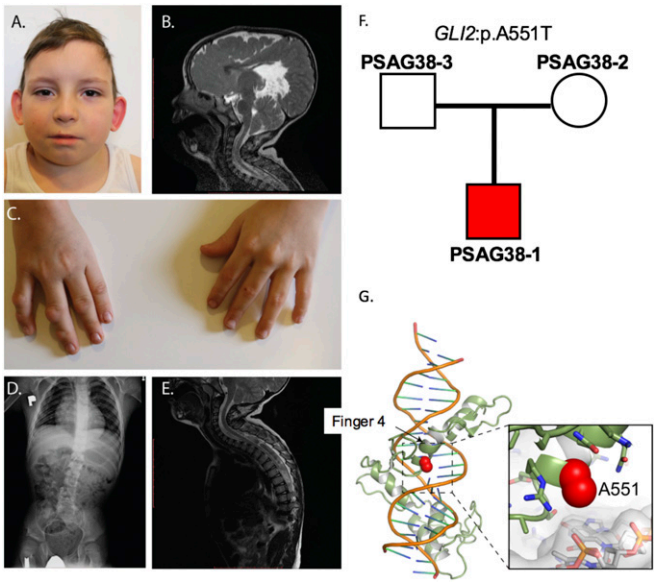

Fig. 2. De novo mutation in *GLI2*. (*A*) The proband at 8 y of age, demonstrating bitemporal narrowing as a result of uncorrected sagittal synostosis. (*B*) T2-weighted MRI demonstrating hydrocephalus, white matter abnormalities, and hypoplasia of the corpus callosum. The patient was also born with right thumb agenesis (*C*) and severe kyphosis and scoliosis (*D* and *E*). Hip dysplasia requiring operative management is also evident at the bottom of *D*. (*F*) The mutation p.A551T in *GLI2* was only present in the proband but not in parents. (*G*) The crystal structure of the paralog GLI1 (18) (PDB ID code 2GLI) is shown, indicating the location of A551 within the major groove-binding Finger 4 motif and abutting the adjacent nucleotide. Structural figures were generated using Pymol (https://pymol.org/2/).

GLI2 is a key mediator of hedgehog signaling, a pathway that has been implicated in cranial suture morphogenesis, brain development, and skeletal patterning (19). GLI2 haploinsufficiency has previously been implicated in a spectrum of phenotypes, including postaxial polydactyly, structural brain abnormalities, hypopituitarism, unusual facial features, delayed growth, facial clefts, and holoprosencephaly (20, 21). The phenotypes of our proband are mostly distinct from those seen in patients with LOF mutations in *GLI2*, although this patient's neurogeneic bladder is consistent with the urogenital anomalies observed in *GLI2* knockout mice (22). The altered binding interaction with DNA raises the possibility that this mutation has complex effects entailing both LOF and neomorphic effects resulting from binding to ectopic DNA sequences; this could account for the distinctive phenotypic features of this patient.

There was a damaging de novo variant in *SOX11* (p.R64H) in a child with unilateral lambdoid synostosis, microgenia, hip dysplasia, lower lip eversion, low-set ears, developmental delay, hypotonia, aplasia of the fifth distal phalanx bilaterally, postaxial polydactyly, and clinodactyly (Fig. 3*A* and *SI Appendix*, Table S2). SOX11 is a transcription factor downstream of BMP signaling previously demonstrated to enhance early osteoblast differentiation by increasing expression of lineage-specific transcription factors RUNX2 and SP7 (23); *SOX11* has a pLI of 0.34. SOX11 is also involved in the embryonic neurogenesis and tissue modeling during development. LOF mutations in *SOX11* have previously been implicated in syndromic intellectual disability resembling Coffin–Siris syndrome, which usually presents with hypotonia, microcephaly, and coarse facial features in addition to severe developmental delay (24).

There is very high sequence identity over 90% between SOX11 and the C-group Sox protein SOX4 (*SI Appendix*, Fig. S1), strongly suggesting that SOX4 and SOX11 fold and bind DNA in a similar manner. Analysis of sequence alignment and the crystal structure of SOX4 bound to DNA (PDB ID code 3U2B) (25) (Fig. 3*C*) indicate that Arg64 should function similarly to the equivalent conserved arginine in SOX4 and SOX17 as a critical residue for DNA sequence recognition (25). Mutation of Arg64 to histidine is, therefore, predicted to significantly impair correct DNA recognition. To our knowledge, the presence of lambdoid CS, postaxial polydactyly, and hip dysplasia has not been reported in association with *SOX11* mutation. While there is overlap of the features of this patient with prior patients with haploinsufficiency for SOX11, the previously unreported features seen in our patient raise the question of whether there might be neomorphic effects of altering the DNA binding specificity of SOX11.

We identified a de novo 15-nucleotide in-frame insertion (p.V374_375insSWKMK) in *CTNNA1*, which encodes an α-catenin protein; α-catenin proteins link the cytoplasmic domain of cadherins to filamentous actins and help stabilize adherens junctions by binding to both filamentous actin and vinculin. They are intricately involved in multiple complexes that regulate cell adhesion and differentiation. The proband was born with polydactyly of the right thumb, a right supernumerary nipple, 3 cartilaginous skin tags

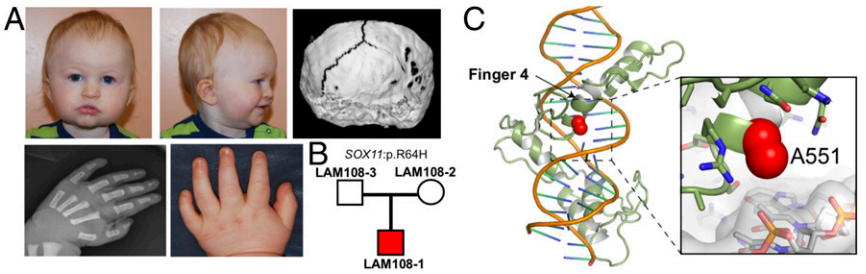

Fig. 3. De novo mutation in *SOX11*. (*A*) Note the full cheeks, everted lower lip, brachydactyly, and clinodactyly (37). Three-dimensional computed tomography reconstruction demonstrates R lambdoid CS. The X-ray of the hand demonstrates absence of the fifth digit distal phalanx. The proband's sixth digit was removed early in infancy and thus, is not shown. (*B*) The mutation p.R64H in *SOX11* was present in the proband but not in parents. (*C*) Analysis of sequence alignment indicates that Arg64 should function similar to the equivalent conserved arginine in SOX4 and SOX17 as a critical residue for DNA sequence recognition (25). Structural analysis of the nearly identical Sox4 in complex with DNA (PDB ID code 3U2B) (25) indicates that arginine at the location of R64 is critical for proper DNA sequence recognition.

around his right ear, tooth enamel defects, a hydrocele, an inguinal hernia, and sagittal CS (*SI Appendix*, Table S2). *CTNNA1* has a pLI of 0.97. The structural basis of autoregulation for α-catenin interaction with vinculin is thought to be mediated by a major conformational change in the vinculin-binding domain (26); the autoinhibited crystal structure of α-catenin shows this domain to be a 4-helix bundle (27), but in its complex with vinculin, this domain is "unfurled" (26). The p.V374_375insSWKMK insert is located in the center of 1 of the α-helices of the vinculin-binding domain (*SI Appendix*, Fig. S2). The insertion is expected to destabilize the helix and consequently, the autoinhibited 4-helix bundle, perhaps resulting in either altered vinculin binding or α-catenin degradation.

Lastly, we identified a hemizygous LOF mutation in *GPC4* (p.V152fs*3), a regulator of Wnt signaling, in a male child with syndromic metopic synostosis (Fig. 4*A*). This mutation was de novo in the proband's mother. *GPC4* has a pLI of 0.95 (Fig. 4*B*). The proband also had severe growth delay with shortened long bones, a single cupped ear, depressed nasal bridge, short nose, amblyopia, nystagmus, and gingival hyperplasia (Fig. 4*A* and *SI Appendix*, Table S2). A proband without CS yet with similar extracranial anomalies resembling Robinow syndrome was recently reported in a child with a hemizygous *GPC4* variant (28). The findings in our proband lend strong support to the existence of an X-linked form of Robinow syndrome occurring via *GPC4* insufficiency. They also lend additional support to the link between cranial suture morphogenesis and regulation of Wnt signaling (3, 29).

We recently described an association between rare, damaging variants in *SMAD6* and midline CS, with penetrance of disease modified by a common risk allele (rs1884302) downstream of *BMP2* (2). We genotyped rs1884302 in these kindreds with syndromic CS and found no significant association between the risk allele and disease ($P = 0.25$, binomial test; "C" risk allele transmitted in 5 of 9 possible heterozygous transmissions). The *BMP2* risk allele was present in a heterozygous ($n = 2$) or homozygous ($n = 1$) state in 3 of 4 probands with syndromic sagittal CS, consistent with an association of this allele to sagittal CS (30).

Discussion

We have found rare damaging mutations in genes that are highly intolerant to LOF in 8 of 12 probands with syndromic CS who had previously negative genetic studies. Four of these mutations were in *TFAP2B*, strongly implicating this gene in syndromic CS. Mutations in *TFAP2B* had previously been implicated in patent ductus arteriosus with limb anomalies, features that were variable among our *TFAP2B*-mutant probands with CS. This finding clearly establishes *TFAP2B* as a syndromic CS gene and underscores the pleiotropy and variable expressivity resulting from haploinsufficiency for this gene.

Among the remaining 8 probands, 5 had de novo damaging mutations, all but 1 in very high pLI genes. Haploinsufficiency for only 1, *KAT6A*, had previously shown any association with CS. Haploinsufficiency for 3 others, *GLI2*, *SOX11*, and *GPC4*, has been associated with other congenital malformations and acts in the Wnt, BMP, and hedgehog signaling pathways in which mutation in other genes has been frequently implicated in syndromic CS. These findings are highly unlikely to have occurred by chance and strongly suggest that the identified mutations are causal to CS in these patients. The significance of mutation in 2 of these genes is further supported by phenotypic overlap of patients harboring these mutations with other patients with mutation in the same genes (*GPC4* and *SOX11*). Lastly, we identified a damaging de novo in-frame insertion within the vinculin-binding domain of *CTNNA1*, potentially implicating another pathway regulating cell differentiation in CS. It would be of interest to determine whether other patients previously shown to have haploinsufficient mutations in these genes have previously unrecognized CS. Additionally, however, 2 of these genes encode transcription factors and had mutations at positions in immediate proximity to sites of interaction with cognate DNA binding sites, raising the possibility that these mutations might impart more complex effects than simple LOF.

Our study of just 12 syndromic CS patients with negative genetic studies for mutations in known CS genes identified 1 statistically significant CS gene (*TFAP2B*), provided confirmation for others (*KAT6A* and *GPC4*), and provided support for the role of 3 others. These findings make clear that additional genes remain to be identified among "mutation-negative" subjects, providing strong motivation to study all such patients. The 3 remaining patients who do not have putative causal mutations are candidates for additional study. Small copy number variants, deep intronic splice mutations, oligogenic inheritance, and environmental phenocopies are all potential explanations. Nevertheless, the high diagnostic rate of these mutation-negative kindreds strongly supports exome sequencing of case-parent trios as the appropriate next step in management for syndromic CS probands without mutations at prevalent syndromic loci (31).

The results also provide continuing evidence (3, 5, 6, 32) of pleiotropy and variable expressivity resulting from mutation in genes in which haploinsufficiency causes disease, with observed

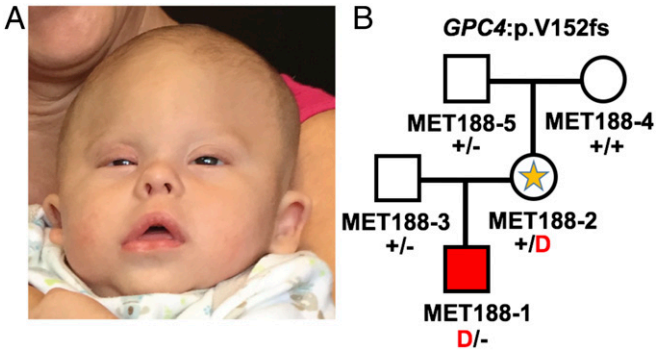

Fig. 4. Proband with hemizygous *GPC4* LOF mutation. (*A*) The images demonstrate trigonocephaly, a depressed nasal bridge, and a cupped right ear. (*B*) Pedigree of family with *GPC4* LOF mutation: + represents a wild-type allele, and D represents the mutant allele of GPC4, p.V152fs. The frameshift mutation was de novo in the affected child's mother as denoted by the star. This mutation was transmitted to her son, who was hemizygous for the *GPC4* LOF mutation. Sanger sequencing traces are shown in *SI Appendix*, Fig. S3.

phenotypes showing incomplete overlap with phenotypes previously associated with damaging mutations in these genes. For example, analysis of 22 individuals from a large kindred harboring the same LOF mutation in *TFAP2B* demonstrated ∼50% penetrance of PDA and 80% penetrance of facial dysmorphology but nearly complete penetrance of clinodactyly; thus, even in the same genetic background, considerable variable expressivity has been observed (14). The findings underscore the role of ascertainment in the phenotypes observed. The striking phenotypic variability could be explained by the effects of variants at other loci, allelic effects, environmental effects, or chance. In nonsyndromic CS, we recently demonstrated the clear role of nonadditive interactions of rare *SMAD6* LOF mutations and a common variant near *BMP2*, with penetrance of CS drastically increasing with the combination of these risk loci over the presence of either alone (2). Interestingly, haploinsufficiency for SMAD6 has also been implicated in congenital heart disease (CHD) (6); none of these patients have had concurrent CS. Thus, it is plausible that the combination of rare alleles with common modifiers at other loci might underlie the phenotypic variability observed in these and other Mendelian disorders. Significant overlap was also recently shown to exist between genes harboring rare mutation with large effect in CHD and autism (6), which might also be explained by modifier loci. These results also comport with findings in CHD in which de novo mutations contribute to ∼3% of probands with isolated CHD but 27% of CHD with complex extracardiac phenotypes (32), emphasizing the high yield for rare mutations with large effect in syndromic patients.

Large-scale exome sequencing projects have been highly successful in identifying genes and pathways implicated in diseases featuring high locus heterogeneity in recent years, including autism (33–36), CHD (6, 7, 32), and CS (2, 3). The identification of a high frequency of damaging mutations in genes highly intolerant to LOF in this small cohort implies that sequencing a substantially larger cohort of mutation-negative syndromic trios will be highly productive in identifying additional loci affecting craniofacial development. We anticipate that similar findings will apply to many other syndromic traits.

Methods

Subjects and Samples. Participants for this study were ascertained from the Yale Pediatric Craniofacial Clinic; from the Pediatric Neurosurgery Clinic at the Medical University of Silesia, Poland; or by responding to an invitation posted on the Cranio Kids–Craniosynostosis Support and Craniosynostosis–Positional Plagiocephaly Support Facebook pages. All participating individuals or their parents provided written informed consent to participate in a study of the genetic cause of CS in their family. Inclusion criteria included a diagnosis of syndromic CS in the absence of known syndromic forms of disease by a craniofacial plastic surgeon or pediatric neurosurgeon. The study protocol was approved by the Yale Human Investigation Committee Institutional Review Board. Patient photographs were used with family permission and were provided by participating families or treating clinicians.

Exome Sequencing and Analysis. DNA was prepared from buccal swab or saliva samples according to the manufacturer's protocol. Exome sequencing was performed by exon capture using the IDT xGen capture reagent followed by 99 base paired end sequencing on the Illumina HiSeq 2000, with variant calls analyzed as previously described (3).

Burden of De Novo Mutations. Statistical analysis of the probability of observing multiple damaging de novo mutations in an individual gene in CS cases was performed in R using the denovolyzeR package as previously described (2, 37). The expected number of de novo mutations in each gene across variant classes was calculated, and this value was compared with the observed number using Poisson statistics (8).

ACKNOWLEDGMENTS. This project was supported by the Yale Center for Mendelian Genomics (NIH Grant M#UM1HG006504-05) and the NIH Medical Scientist Training Program (NIH/National Institute of General Medical Sciences Grant T32GM007205).

1. S. R. Twigg, A. O. Wilkie, A genetic-pathophysiological framework for craniosynostosis. *Am. J. Hum. Genet.* **97**, 359–377 (2015).
2. A. T. Timberlake *et al*., Two locus inheritance of non-syndromic midline craniosynostosis via rare *SMAD6* and common *BMP2* alleles. *eLife* **5**, e20125 (2016).
3. A. T. Timberlake *et al*., De novo mutations in inhibitors of Wnt, BMP, and Ras/ERK signaling pathways in non-syndromic midline craniosynostosis. *Proc. Natl. Acad. Sci. U.S.A.* **114**, E7341–E7347 (2017).
4. A. O. M. Wilkie, D. Johnson, S. A. Wall, Clinical genetics of craniosynostosis. *Curr. Opin. Pediatr.* **29**, 622–628 (2017).
5. C.G. Furey *et al*., De novo mutation in genes regulating neural stem cell fate in human congenital hydrocephalus. *Neuron* **99**, 302–314.e4 (2018).
6. S. C. Jin *et al*., Contribution of rare inherited and de novo variants in 2,871 congenital heart disease probands. *Nat. Genet.* **49**, 1593–1601 (2017).
7. S. Zaidi *et al*., De novo mutations in histone-modifying genes in congenital heart disease. *Nature* **498**, 220–223 (2013).
8. K. E. Samocha *et al*., A framework for the interpretation of de novo mutation in human disease. *Nat. Genet.* **46**, 944–950 (2014).
9. M. Lek *et al*.; Exome Aggregation Consortium, Analysis of protein-coding genetic variation in 60,706 humans. *Nature* **536**, 285–291 (2016).
10. Y. Komatsu *et al*., Augmentation of Smad-dependent BMP signaling in neural crest cells causes craniosynostosis in mice. *J. Bone Miner. Res.* **28**, 1422–1433 (2013).
11. Y. Mishina, T. N. Snider, Neural crest cell signaling pathways critical to cranial bone development and pathology. *Exp. Cell Res.* **325**, 138–147 (2014).
12. M. Ishii, J. Sun, M. C. Ting, R. E. Maxson, The development of the calvarial bones and sutures and the pathophysiology of craniosynostosis. *Curr. Top. Dev. Biol.* **115**, 131–156 (2015).
13. M. Satoda *et al*., Mutations in TFAP2B cause Char syndrome, a familial form of patent ductus arteriosus. *Nat. Genet.* **25**, 42–46 (2000).
14. A. Mani *et al*., Syndromic patent ductus arteriosus: Evidence for haploinsufficient TFAP2B mutations and identification of a linked sleep disorder. *Proc. Natl. Acad. Sci. U.S.A.* **102**, 2975–2979 (2005).
15. V. A. Arboleda *et al*.; UCLA Clinical Genomics Center, De novo nonsense mutations in KAT6A, a lysine acetyl-transferase gene, cause a syndrome including microcephaly and global developmental delay. *Am. J. Hum. Genet.* **96**, 498–506 (2015).
16. E. Tham *et al*., Dominant mutations in KAT6A cause intellectual disability with recognizable syndromic features. *Am. J. Hum. Genet.* **96**, 507–513 (2015).
17. S. M. Shimeld, C2H2 zinc finger genes of the Gli, Zic, KLF, SP, Wilms' tumour, Huckebein, Snail, Ovo, Spalt, Odd, Blimp-1, Fez and related gene families from Branchiostoma floridae. *Dev. Genes Evol.* **218**, 639–649 (2008).
18. N. P. Pavletich, C. O. Pabo, Crystal structure of a five-finger GLI-DNA complex: New perspectives on zinc fingers. *Science* **261**, 1701–1707 (1993).
19. A. Pan, L. Chang, A. Nguyen, A. W. James, A review of hedgehog signaling in cranial bone development. *Front. Physiol.* **4**, 61 (2013).
20. K. A. Bear *et al*., Pathogenic mutations in GLI2 cause a specific phenotype that is distinct from holoprosencephaly. *J. Med. Genet.* **51**, 413–418 (2014).
21. F. L. Culler, K. L. Jones, Hypopituitarism in association with postaxial polydactyly. *J. Pediatr.* **104**, 881–884 (1984).
22. R. Haraguchi *et al*., Molecular analysis of coordinated bladder and urogenital organ formation by Hedgehog signaling. *Development* **134**, 525–533 (2007).
23. J. Gadi *et al*., The transcription factor protein Sox11 enhances early osteoblast differentiation by facilitating proliferation and the survival of mesenchymal and osteoblast progenitors. *J. Biol. Chem.* **288**, 25400–25413 (2013).
24. Y. Tsurusaki *et al*., De novo SOX11 mutations cause Coffin-Siris syndrome. *Nat. Commun.* **5**, 4011 (2014).
25. R. Jauch, C. K. Ng, K. Narasimhan, P. R. Kolatkar, The crystal structure of the Sox4 HMG domain-DNA complex suggests a mechanism for positional interdependence in DNA recognition. *Biochem. J.* **443**, 39–47 (2012).
26. E. S. Rangarajan, T. Izard, The cytoskeletal protein α-catenin unfurls upon binding to vinculin. *J. Biol. Chem.* **287**, 18492–18499 (2012).
27. N. Ishiyama *et al*., An autoinhibited structure of α-catenin and its implications for vinculin recruitment to adherens junctions. *J. Biol. Chem.* **288**, 15913–15925 (2013).
28. J. J. White *et al*.; Baylor-Hopkins Center for Mendelian Genomics, WNT signaling perturbations underlie the genetic heterogeneity of Robinow syndrome. *Am. J. Hum. Genet.* **102**, 27–43 (2018).
29. H. M. Yu *et al*., The role of Axin2 in calvarial morphogenesis and craniosynostosis. *Development* **132**, 1995–2005 (2005).
30. C. M. Justice *et al*., A genome-wide association study identifies susceptibility loci for nonsyndromic sagittal craniosynostosis near BMP2 and within BBS9. *Nat. Genet.* **44**, 1360–1364 (2012).
31. K. A. Miller *et al*., Diagnostic value of exome and whole genome sequencing in craniosynostosis. *J. Med. Genet.* **54**, 260–268 (2017).
32. J. Homsy *et al*., De novo mutations in congenital heart disease with neurodevelopmental and other congenital anomalies. *Science* **350**, 1262–1266 (2015).
33. S. De Rubeis *et al*.; DDD Study; Homozygosity Mapping Collaborative for Autism; UK10K Consortium, Synaptic, transcriptional and chromatin genes disrupted in autism. *Nature* **515**, 209–215 (2014).
34. I. Iossifov *et al*., The contribution of de novo coding mutations to autism spectrum disorder. *Nature* **515**, 216–221 (2014).
35. I. Iossifov *et al*., De novo gene disruptions in children on the autistic spectrum. *Neuron* **74**, 285–299 (2012).
36. B. J. O'Roak *et al*., Exome sequencing in sporadic autism spectrum disorders identifies severe de novo mutations. *Nat. Genet.* **43**, 585–589 (2011).
37. J. S. Ware, K. E. Samocha, J. Homsy, M. J. Daly, Interpreting de novo variation in human disease using denovolyzeR. *Curr. Protoc. Hum. Genet.* **87**, 7.25.1–7.25.15 (2015).

Correction

GENETICS

Correction for "Mutations in *TFAP2B* and previously unimplicated genes of the BMP, Wnt, and Hedgehog pathways in syndromic craniosynostosis," by Andrew T. Timberlake, Sheng Chih Jin, Carol Nelson-Williams, Robin Wu, Charuta G. Furey, Barira Islam, Shozeb Haider, Erin Loring, Amy Galm, Yale Center for Genome Analysis, Derek M. Steinbacher, Dawid Larysz, David A. Staffenberg, Roberto L. Flores, Eduardo D. Rodriguez, Titus J. Boggon, John A. Persing, and Richard P. Lifton, which was first published July 10, 2019; 10.1073/pnas.1902041116 (*Proc. Natl. Acad. Sci. U.S.A.* **116**, 15116–15121).

The authors note that Fig. 3 appeared incorrectly. The corrected figure and its legend appear below.

The authors also note that, due to a printer's error, Table 2 appeared incorrectly. The corrected table appears below.

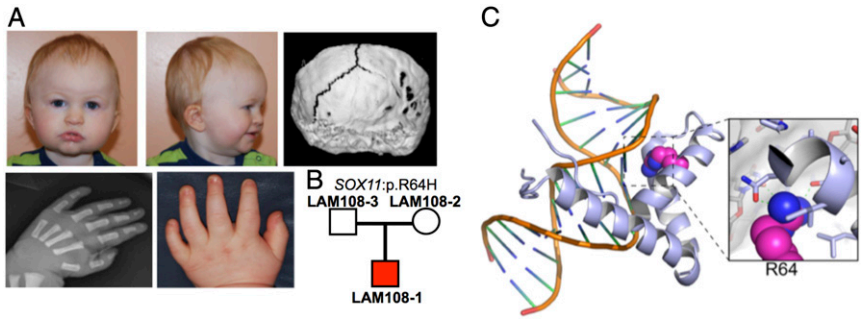

Fig. 3. De novo mutation in *SOX11*. (*A*) Note the full cheeks, everted lower lip, brachydactyly, and clinodactyly (37). Three-dimensional computed tomography reconstruction demonstrates R lambdoid CS. The X-ray of the hand demonstrates absence of the fifth digit distal phalanx. The proband's sixth digit was removed early in infancy and thus, is not shown. (*B*) The mutation p.R64H in *SOX11* was present in the proband but not in parents. (*C*) Analysis of sequence alignment indicates that Arg64 should function similar to the equivalent conserved arginine in SOX4 and SOX17 as a critical residue for DNA sequence recognition (25). Structural analysis of the nearly identical Sox4 in complex with DNA (PDB ID code 3U2B) (25) indicates that arginine at the location of R64 is critical for proper DNA sequence recognition.

Table 2. Likely pathogenic variants in probands with syndromic CS

Kindred identification	Type of CS	Gene	Impact	Inheritance	ExAC frequency	pLI
SAG249	Sagittal	*TFAP2B*	M1I (start loss)	Inherited (unaffected parent)	0	0.99
MET268	Metopic	*TFAP2B*	K276R	De novo	0	0.99
MET271	Metopic	*TFAP2B*	IVS3+2 T > A	De novo	0	0.99
MET117	Metopic	*TFAP2B*	R382X	Inherited (affected parent)	0	0.99
SAG250	Sagittal and metopic	*KAT6A*	E1221X	De novo	0	1
LAM108	Lambdoid	*SOX11*	R64H	De novo	0	0.34
PSAG38	Sagittal	*GLI2*	A551T	De novo	0	1
MET188	Metopic	*GPC4*	V152fs	De novo in mother	0	0.95
SAG359	Sagittal	*CTNNA1*	V374_375insSWKMK	De novo	0	0.97

Published online August 12, 2019.

www.pnas.org/cgi/doi/10.1073/pnas.1912893116